Tripartite structure of *Saccharomyces cerevisiae* Dna2 helicase/endonuclease

Sung-Ho Bae, Jung-Ae Kim, Eunju Choi, Kyoung-Hwa Lee, Ho-Young Kang, Hee-Dai Kim, Jae-Hoon Kim, Kwang-Hee Bae, Yunje Cho[1], Chankyu Park[2] and Yeon-Soo Seo*

National Creative Research Initiative Center for Cell Cycle Control, Samsung Biomedical Research Institute, Sungkyunkwan University School of Medicine, 300 Chunchun-Dong, Changan-Ku, Suwon, Kyunggi-Do 440-746, Korea, [1]Department of Life Science, and Division of Molecular and Life Science, Pohang University of Science and Technology, Pohang, Kyungbuk 790-784, Korea and [2]Department of Biological Sciences, Korea Advanced Institute of Science and Technology, Yusung-Ku, Taejon 305-701, Korea

ABSTRACT

In order to gain insights into the structural basis of the multifunctional Dna2 enzyme involved in Okazaki fragment processing, we performed biochemical, biophysical and genetic studies to dissect the domain structure of Dna2. Proteolytic digestion of Dna2 using subtilisin produced a 127 kDa polypeptide that lacked the 45 kDa N-terminal region of Dna2. Further digestion generated two subtilisin-resistant core fragments of approximately equal size, 58 and 60 kDa. Surprisingly, digestion resulted in a significant (3- to 8-fold) increase in both ATPase and endonuclease activities compared to the intact enzyme. However, cells with a mutant *DNA2* allele lacking the corresponding N-terminal region were severely impaired in growth, being unable to grow at 37°C, indicating that the N-terminal region contains a domain critical for a cellular function(s) of Dna2. Analyses of the hydrodynamic properties of and *in vivo* complex formation by wild-type and/or mutant Dna2 lacking the N-terminal 45 kDa domain revealed that Dna2 is active as the monomer and thus the defect in the mutant Dna2 protein is not due to its inability to multimerize. In addition, we found that the N-terminal 45 kDa domain interacts physically with a central region located between the two catalytic domains. Our results suggest that the N-terminal 45 kDa domain of Dna2 plays a critical role in regulation of the enzymatic activities of Dna2 by serving as a site for intra- and intermolecular interactions essential for optimal function of Dna2 in Okazaki fragment processing. The possible mode of regulation of Dna2 is discussed based upon our recent finding that replication protein A interacts functionally and physically with Dna2 during Okazaki fragment processing.

INTRODUCTION

DNA2 encodes a 172 kDa protein that is a multifunctional enzyme and thus has been implicated in several different aspects of DNA transactions (1–6). Immunoaffinity-purified Dna2 fusion protein from crude extracts displayed single-stranded (ss)DNA-dependent ATPase and DNA helicase activities (2,7). Recombinant Dna2 isolated from insect cells was shown to possess intrinsic ssDNA-specific endonuclease activity in addition to helicase activity (7). The conserved amino acid residues essential for endonuclease activity located in the middle part of Dna2 do not overlap with the helicase motifs in the C-terminal one-third of the enzyme (8–10). The genetic and physical interactions of Dna2 with Rad27 (a yeast homolog of mammalian Fen1) suggest that Dna2 may play a role in Okazaki fragment metabolism (11). Consistent with this, *in vivo* and *in vitro* analyses of *dna2* temperature-sensitive mutant alleles showed that Dna2 is likely to be involved in lagging strand synthesis (12–14). For example, *dna2* and *rad27*Δ mutant strains contain DNA lesions that are predicted to occur in strains with aberrant lagging strand synthesis (14). Recently, we discovered that the endonuclease activity associated with Dna2 preferentially cleaves ssDNA with free ends and that the helicase activity unwinds duplex DNA in the 5′→3′ direction (1). The cleavage reaction was stimulated by the presence of an RNA segment at the 5′-end of flap DNA. The 5′-end region of Okazaki fragments is efficiently processed by Dna2 when it is displaced from the template by the DNA polymerase (pol) δ extending the upstream primer (1). These enzymatic properties of Dna2 provided a biochemical basis for a role in Okazaki fragment maturation (1). Consistent with these *in vitro* findings, the *dna2*+ gene of *Schizosaccharomyces pombe* interacts either genetically or physically with two subunits (*cdc1*+ and *cdc27*+) of pol δ, *rad2*+ (the *S.pombe* homolog of mammalian Fen1) and *cdc17*+ (DNA ligase I), all of which are required for Okazaki fragment maturation (5).

In addition to its role in Okazaki fragment processing, Dna2 may have other roles during DNA replication. This probability is based on the following observations. First, *DNA2* was found to genetically interact with *POL1* through *CTF4*, which encode DNA pol α and a DNA pol α-associated protein,

*To whom correspondence should be addressed. Tel: +82 31 299 6440; Fax: +82 31 299 6435; Email: ysseo@med.skku.ac.kr

respectively (4). Thus Dna2 is likely to be involved in each new Okazaki fragment synthesis. Secondly, initiation of DNA replication was significantly impaired upon depletion of XDna2 in *Xenopus* egg extracts (6). Thirdly, the *dna2-1* mutation was synthetically lethal when combined with *mcm10*, which is known to be involved in initiation of chromosomal DNA replication (6). Furthermore, Dna2 may play a role(s) in either DNA repair or recombination. Several of the mutant alleles of *DNA2* isolated to date render cells sensitive to various mutagenic agents, such as methylmethane sulfonate (MMS) and exposure to X-rays (3,4). Furthermore, a *dna2*Δ strain that was kept viable by overproducing Rad27 was highly sensitive to UV (3). These observations suggest that Dna2 is involved in post-replication and double-strand break repair pathways (3). *In vivo* and *in vitro* interaction studies also demonstrate that Dna2 interacts with Rdh54, a protein implicated in both recombination and repair (I.Stagljar, personal communication). Thus, Dna2 appears to be involved in a number of DNA transactions, presumably through multiple protein–protein interactions that may regulate the diverse *in vivo* functions of Dna2. In addition, changes in expression levels of Dna2 affected cell growth and gene expression (11,14,15). Overexpression of full-length Dna2 caused arrest of cell growth (14), an effect that is not observed when a truncated Dna2 protein lacking the N-terminal 105 amino acids was overexpressed (11). Moreover, overexpression of an N-terminal portion of Dna2 causes significant derepression of a gene located near a telomere in yeast (15), indicating that the N-terminal part of Dna2 may play a unique or regulatory role in DNA transactions.

In order to understand the structural basis that accounts for the multifunctional nature of Dna2 *in vivo*, we dissected the domain structure of the Dna2 protein *in vitro*. In this report we present evidence that the N-terminal region is critical for the regulation or proper implementation of the enzymatic activities of Dna2 by providing a site for protein–protein interactions required for its concerted action with other replication proteins.

MATERIALS AND METHODS

Oligonucleotides, plasmids, nucleoside triphosphates and enzymes

All oligonucleotides used to construct various DNA substrates were synthesized commercially (Genotech, Taejeon, Korea) and gel-purified prior to use. Nucleoside triphosphates were obtained from Boehringer Mannheim and [γ-^{32}P]ATP (>5000 Ci/mmol) and [α-^{32}P]dCTP (>6000 Ci/mmol) were purchased from Amersham Pharmacia Biotech. Restriction endonucleases and the Klenow fragment of *Escherichia coli* DNA polymerase I were purchased from Promega. Subtilisin was obtained from Sigma. The pRS series and pYES2 plasmids were purchased from New England Biolabs and Invitrogen, respectively.

Purification of recombinant Dna2 proteins HX-Dna2, HX-Dna2Δ405N, HX-Dna2N and HA-Dna2 in insect cells

Recombinant Dna2 proteins including HX-Dna2 (wild-type) and HX-Dna2Δ405N (lacking the N-terminal 405 amino acids) were expressed in insect cells and purified as described (7). In order to prepare HX-Dna2N (a truncated protein containing the

N-terminal 405 amino acids of Dna2), the *Bam*HI–*Nde*I fragment (blunt ended with T4 DNA pol) from pHX-DNA2 (7) was cloned into the *Bam*HI and *Eco*RI sites of pBlueBacHis2A (blunt ended with T4 DNA pol) (Invitrogen). In order to prepare hemagglutinin epitope-tagged Dna2 (HA-Dna2), two oligonucleotides (5′-G ATC **ATG** TAC CCA TAC GAC GTT CCA GAT TAC GCT G-3′ and 5′-GA TCC AGC GTA ATC TGG AAC GTC GTA TGG GTA **CAT**-3′) were annealed and inserted into the *Bam*HI site of pFastBac1 (Life Technologies) to create a new start codon (bold) and hemagglutinin epitope (underlined). The *Bam*HI fragment from pHX-Dna2, containing the entire open reading frame of the *DNA2* gene, was subcloned into the resulting pFastBac1 derivative to obtain pHA-DNA2. Recombinant baculoviruses were constructed as recommended by the manufacturers. All recombinant proteins except HA-Dna2 contained an additional 37 amino acids (MPRGS **HHHHH** HGMAS MTGGQ QMGRD LYDDD DKDRW GS) at their N-termini. These included six histidines (bold) and the Xpress epitope (underlined) fused to its N-terminal methionine to facilitate detection and purification of the recombinant Dna2 proteins. HX-Dna2N behaved similarly to HX-Dna2 in chromatographic steps and was purified using the same procedure described for HX-Dna2 (7).

Preparation of the endonuclease substrate

A DNA substrate used to examine endonuclease activity of the Dna2 proteins was prepared by hybridizing a 73mer to ΦX174 sscDNA as described (7). The substrate contains a free 21 nt ssDNA 5′-tail connected to a 52 bp duplex. The 3′-ends of the annealed oligonucleotides were labeled by incorporating [α-^{32}P]dCTP, chased with excess cold dCTP in the presence of the Klenow fragment. The substrate was purified prior to use as described (16), and had a specific activity of ~3000 c.p.m./fmol.

ATPase and endonuclease assays

Standard assays for measuring ssDNA-dependent ATPase activity were carried out in a reaction mixture (20 μl) containing 50 mM Tris–HCl, pH 7.8, 0.3 mM MgCl$_2$, 2 mM dithiothreitol (DTT), 0.25 mg/ml bovine serum albumin (BSA), 150 μM cold ATP, 20 nM [γ-^{32}P]ATP (>5000 Ci/mmol) and 50 ng M13 sscDNA. After incubation at 37°C for 10 min, an aliquot (2 μl) was spotted onto a polyethyleneimine–cellulose plate (J. T. Baker Inc.), which was then developed in 0.5 M LiCl/1.0 M formic acid solution. The products were analyzed using a PhosphorImager (Molecular Dynamics).

The reaction mixture (20 μl) used to examine endonuclease activity contained 50 mM Tris–HCl, pH 7.8, 5 mM MgCl$_2$, 2 mM DTT, 0.25 mg/ml BSA and the 3′-^{32}P-labeled partial duplex ΦX174 DNA substrate (15 fmol). After incubation at 37°C for 5 min, reactions were stopped with 4 μl of 6× stop solution (60 mM EDTA, pH 8.0, 40% w/v sucrose, 0.6% SDS, 0.25% bromophenol blue and 0.25% xylene cyanol). The cleavage products were boiled and then subjected to electrophoresis on a 10% polyacrylamide gel containing 0.1% SDS in 0.5× TBE (45 mM Tris base, 45 mM boric acid and 1 mM EDTA). The amounts of products formed were measured using a PhosphorImager (Molecular Dynamics).

Polyclonal antibodies against HX-Dna2 and HX-Dna2N

The polyclonal antibody against full-length HX-Dna2 protein, anti-Dna2, was as described (7). The glycerol gradient fraction

Table 1. *Saccharomyces cerevisiae* strains used in this study

Strain	Genotype
YPH499	MAT**a**, *ade2, ura3, lys2, trp1, his3, leu2, GAL+*
YPH501	MAT**a**/α, *ade2, ura3, lys2, trp1, his3, leu2, GAL+*
YKH12	MAT**a**, *ade2, ura3, lys2, trp1, his3, leu2, GAL+, pRS316-DNA2*
YJA2	MAT**a**, *ade2, ura3, lys2, trp1, his3, leu2, GAL+, dna2Δ::dna2Δ405N*
YJA7	MAT**a**, *ade2, ura3, lys2, trp1, his3, leu2, GAL+, dna2Δ::dna2Δ105N*

Table 2. Plasmids used in this study

Plasmid	Description of insert	Selectable marker
pRS316-DNA2	Promoter[a] + *DNA2*	*URA3*
pRS306-dna2Δ105N	Promoter + *dna2Δ105N*	*URA3*
pRS306-dna2Δ405N	Promoter + *dna2Δ405N*	*URA3*
pRS314-DNA2	Promoter + *DNA2*	*TRP1*
pRS314-dna2Δ105N	Promoter + *dna2Δ105N*	*TRP1*
pRS314-dna2Δ405N	Promoter + *dna2Δ405N*	*TRP1*
pRS314-dna2Δ550N	Promoter + *dna2Δ550*	*TRP1*
pYES2-DNA2	GAL promoter–*DNA2*	*URA3*
pYES2-dna2Δ405N	GAL promoter GAL–*dna2Δ405N*	*URA3*
pYES2-dna2N	GAL promoter GAL–*dna2N*	*URA3*
pYES2-RAD27	GAL promoter GAL–*RAD27*	*URA3*

[a]Containing the 397 bp upstream 5′-region of *DNA2* amplified by PCR using the primers described previously (7).

containing 2 mg HX-Dna2N purified from insect cells was used to prepare a polyclonal antibody, α-Dna2N, specific for the N-terminal 405 amino acids of Dna2. The α-Dna2N antibodies did not cross-react with either purified HX-Dna2Δ405N or other proteins present in crude extracts used to purify the N-terminal 405 amino acid fragment of Dna2.

Construction of plasmids and yeast strains

The strains and plasmids constructed are listed in Tables 1 and 2. In order to construct *dna2Δ105N* and *dna2Δ550N* mutant alleles, containing N-terminal 105 and 550 amino acid deletions of *DNA2*, respectively, two PCR primers (5′-CGC <u>GGA TCC</u> **ATG** TCT AAT TTG AGT AGG CA-3′ and 5′-CG<u>G GAT CCA</u> **TG**C AAG ACT CAA TC-3′) were used to create a *Bam*HI site (underlined) and a new start codon (bold) in the *DNA2* gene. The fragments amplified with these and appropriate downstream primers were swapped for the normal N-terminal region of *DNA2* present in pHX-DNA2 (7) to generate *dna2Δ105N* and *dna2Δ550N*. In order to construct *dna2Δ405N*, containing an N-terminal 405 amino acid deletion, two oligonucleotides (5′-TAC AGC GCA CCG <u>GGA TCC</u> **ATG**-3′ and 5′-TA<u>C AT</u>G GAT CCC GGT GCG CTG-3′) were prepared to introduce a new *Bam*HI site (underlined) and

a start codon (bold) in place of Ala[405]. The two oligonucleotides were annealed and inserted directly into pHX-DNA2 cleaved with *Nde*I. The *Bam*HI fragments from the resulting plasmids contain DNA fragments lacking either 105, 405 or 550 N-terminal amino acids of *DNA2*. These plasmids were used for subsequent cloning of N-terminal deleted versions of *DNA2* into appropriate vectors as described below. All plasmids listed in Table 2 contain either the 397 bp promoter sequence of *DNA2* (for pRS derivatives) or the *GAL* promoter (for pYES2 derivatives) and the *Bam*HI sites were used to clone the various *DNA2* genes. Plasmid pYES2-dna2N, containing the N-terminal 405 amino acids of Dna2, was constructed by ligating the *Bam*HI–*Nde*I (blunt ended) fragment from pHX-DNA2 into the *Bam*HI and *Eco*RI sites of pYES2 (blunt ended). The *Eco*RI fragment from pRAD27 (17) containing the entire open reading frame of yeast *RAD27* was inserted into pYES2 to generate pYES2-RAD27.

YKH12, A *dna2*-null yeast strain with an episomal *DNA2* gene is described elsewhere (10). Strains YJA2 and YJA7 were constructed by two-step gene replacement methods. Strain YPH499 was transformed with pRS306-dna2Δ405N and pRS306-dna2Δ105N, followed by selection for Ura+. The transformants were plated on complete synthetic medium (SD) containing 1% 5′-fluoroorotic acid (5′-FOA) to select for cells that had lost the vector sequence, including the Ura+ marker. The authenticity of strains with correct integration of the N-terminal 105 or 405 amino acid-deleted *DNA2* alleles (YJA7 and YJA2, respectively) was confirmed by both PCR and Southern blotting analyses.

Yeast two-hybrid and BIAcore analyses

The *Bam*HI–*Nde*1 fragment (nucleotides 1–1214, see Fig. 7A) containing the N-terminal 405 amino acids of *DNA2* was cloned into pAS2-1 (Clontech) for *GAL4* DNA-binding domain fusion. Six different fragments were prepared using the restriction enzymes as indicated in Figure 7A and cloned into pACT2 (Clontech) for *GAL4* activation domain fusion.

Physical interaction between the N-terminal 45 kDa domain (HX-Dna2N) and HX-Dna2Δ405N was measured by surface plasmon resonance analyses using BIAcore equipment (Pharmacia). ΔRU, the change in refractory index units (RU), was monitored over time after injection of protein solutions onto a Biosensor chip with 2700 RU of immobilized 405 amino acid N-terminal fragment of Dna2, HX-Dna2N. BSA was used as a negative control.

Determination of the assembly states of HX-Dna2 and HX-Dna2Δ405N

Sedimentation values were determined by glycerol gradient centrifugation (5 ml, 15–35% glycerol in buffer T: 25 mM Tris–HCl, pH 7.5, 1 mM EDTA, 10% glycerol, 1 mM DTT, 0.1 mM PMSF, 0.15 μg/ml leupeptin and antipain) in the presence of 500 mM NaCl and 0.02% NP-40. The gradients were centrifuged for 24 h at 48 000 r.p.m. in a Beckman SW55 Ti rotor. Fractions (220 μl) were collected from the bottom of gradients and assayed for ssDNA-dependent ATPase and endonuclease activities. The Stokes radius was determined by gel filtration using a Superose-6 PC 3.2/30 column (SMART system; Amersham Pharmacia). The column was equilibrated with buffer T containing 500 mM NaCl and 0.02% NP-40. The column was calibrated several times to ensure that the marker

proteins were reproducibly eluted at the same position. The fractions collected were assayed for ssDNA-dependent ATPase and endonuclease activities and the Stokes radius of each protein was obtained by plotting $(-\log K_{av})^{1/2}$ against marker proteins. The native molecular weights of HX-Dna2 and HX-Dna2Δ405N were calculated according to Siegel and Monty (18).

RESULTS

Dna2 is activated by proteolytic digestion of the N-terminal 45 kDa domain

In order to gain insights into the relationship between the structure and multiple functions of Dna2, we carried out proteolytic digestion of full-length Dna2 with increasing amounts of subtilisin (Fig. 1A). Treatment of HX-Dna2 with a low level of subtilisin (0.1 μg) mainly produced a polypeptide of 127 kDa (Fig. 1A, lane 2). At higher concentrations (0.2 μg) of subtilisin the intensity of the 127 kDa band decreased markedly, with a concomitant increase in the doublet bands containing polypeptides of 60 and 58 kDa (Fig. 1A, lane 3). This relationship suggests a substrate–product relationship between these polypeptides. Most likely, the two smaller polypeptide products arose from an internal cleavage within the 127 kDa polypeptide.

Western blot analyses with polyclonal antibodies (α-Dna2) raised against full-length HX-Dna2 (7) detected all three proteolytic products (Fig. 1A, lanes 4–6, α-Dna2). In order to define the region of Dna2 that was removed during subtilisin treatment, we determined the N-terminal amino acid sequence of the 127 kDa polypeptide. This analysis revealed multiple amino acids at each position, Thr/His/Lys/Gly, Asp/Phe, Ser/Ala, Thr/Glu/Ile, Leu/Lys and Ser/Asn/Thr, as shown in Figure 1B. The heterogeneity found at each position most likely indicates that the N-terminal ends of the proteolyzed 127 kD product were not uniform. Among 288 combinations of possible sequences, the only sequence that had a match within the entire *DNA2* open reading frame was $_{399}$Thr-Asp-Ser-Thr-Leu-Ser$_{404}$ (Fig. 1B, bold). This indicates that the N-terminal region of Dna2, extending to amino acid 398, was preferentially removed during digestion with subtilisin. In support of this, polyclonal antibodies (α-Dna2N) which recognized only the N-terminal 405 amino acids failed to detect any of the proteolyzed products (Fig. 1A, lanes 7–9, α-Dna2N).

Surprisingly, the proteolyzed products retained both ATPase and endonuclease activities, as shown in Figure 1C and D. The ssDNA-dependent ATPase activity of HX-Dna2 treated with 0.1 μg subtilisin was significantly higher (3- to 8-fold) than the activity of the untreated Dna2 protein control (Fig. 1C). Similar results were obtained for endonuclease activity (measured by cleavage of the ssDNA 5′-tail present in the partial duplex ΦX174 sscDNA substrate) (Fig. 1D). The increase in endonuclease and ATPase activities of Dna2 upon subtilisin digestion is not due to contaminating activities present in subtilisin, since it did not contain any detectable ATPase or endonuclease activity (data not shown). The enzymatic activities associated with the 58 and 60 kDa polypeptides were still more active than that observed with the untreated control, but lower than those of the 127 kDa enzyme (Fig. 1C and D). The fact that the mixture of 58 and 60 kDa polypeptides retained
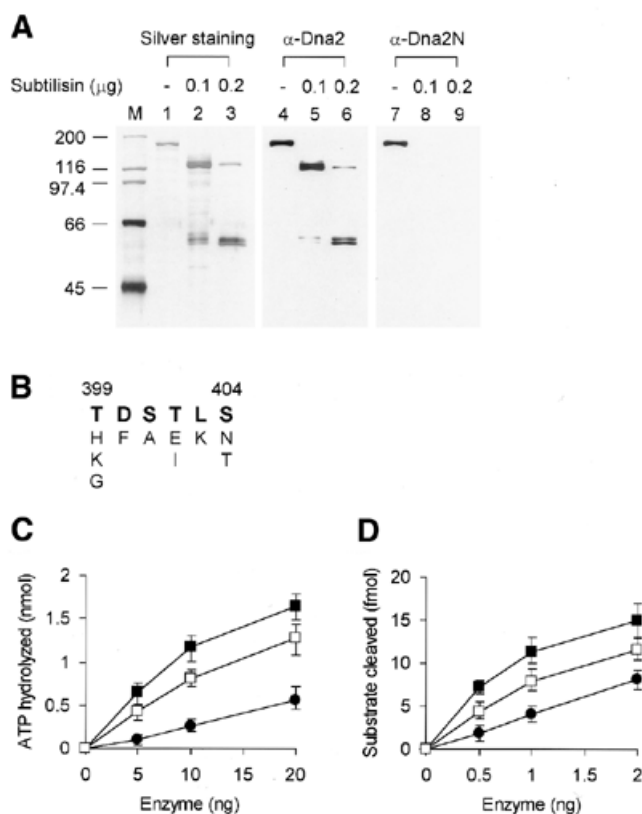
Figure 1. Subtilisin selectively degrades the N-terminal region of Dna2. (**A**) The glycerol gradient fraction of HX-Dna2 enzyme (0.5 mg/ml, 0.2 ml) (7) was incubated with two different concentrations (0.1 and 0.2 μg) of subtilisin at 37°C for 15 min and then analyzed by 10% SDS–PAGE. The glycerol gradient fractions contained 25 mM Tris–HCl, pH 7.8, 1 mM EDTA, 1 mM DTT, 25% glycerol and 0.5 M NaCl. Aliquots containing 0.5 μg Dna2 were subjected to 10% SDS−PAGE and then silver stained or analyzed by western blot analyses using α-Dna2 polyclonal antibodies against full-length HX-Dna2 or α-Dna2N polyclonal antibodies against the N-terminal 405 amino acid fragment. M denotes marker proteins and the numbers on the left indicate the molecular size (kDa). (**B**) Amino acid sequence of the N-terminus of the 127 kDa polypeptide after subtilisin digestion. The sequence matching amino acids 399−404 in the *DNA2* open reading frame is indicated in bold. (**C** and **D**) The digested enzymes were assayed for ATPase (C) and endonuclease (D) activities as described in Materials and Methods. Squares denote HX-Dna2 treated with 0.1 (filled) and 0.2 (open) μg subtilisin. Filled circles represent the activity obtained with an untreated HX-Dna2 control incubated in the absence of subtilisin.

both endonuclease and ATPase activities suggests that each may contain one of the two catalytic activities of Dna2. However, attempts to separate the 58 and 60 kDa polypeptides using a number of purification procedures failed (data not shown). Possibly, these two polypeptides form a tight complex with each other, which is essential for both enzymatic activities. Consistent with this notion, it was reported that the N-terminal 120 kDa and C-terminal 65 kDa truncated fragments did not possess any enzymatic activity (9).

We examined the rate of digestion of HX-Dna2 (100 μg) with subtilisin (0.2 μg) and changes in enzymatic activities of Dna2. Both ATPase and endonuclease activities increased concurrently with the increase in formation of the 127 kDa polypeptide (data not shown), verifying that the subtilisin-generated 127 kDa polypeptide is most active.
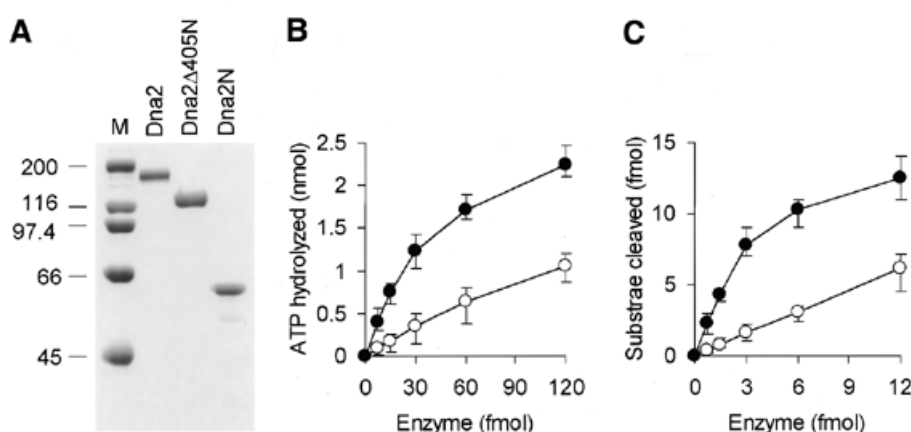
Figure 2. Removal of the N-terminal 405 amino acids activates the enzymatic activities of Dna2. (**A**) Purified HX-Dna2Δ405N was analyzed by 8% SDS–PAGE alongside purified HX-Dna2 and HX-Dna2N. Each lane contained 4 μg purified protein and the gel was subsequently stained with Coomassie brilliant blue. M denotes marker proteins and the numbers on the left of the figure indicate the molecular size (kDa). (**B** and **C**) ATPase (B) and endonuclease (C) activities of HX-Dna2Δ405N (filled circle) and HX-Dna2 (open circle). The amount (fmol) of enzyme added is indicated at the bottom of the graph.

Table 3. Hydrodynamic properties of Dna2 and Dna2Δ405

Enzyme	Calculated monomeric mol. wt (kDa)	Determined native mol. wt[a] (kDa)	Frictional ratio[a] (f/f_o)
HX-Dna2	178	179	1.99
HX-Dna2Δ405N	127	108	1.34

[a]Using the sedimentation coefficients and Stokes radii values obtained in Figure 3, the native molecular weights and the frictional ratios (f/f_o) of HX-Dna2 and HX-Dna2Δ405N were determined using the equations described by Siegel and Monty (18).

Deletion of the N-terminal 405 amino acids is necessary and sufficient for elevated enzyme activity

In order to unambiguously demonstrate that removal of the N-terminal 45 kDa domain of Dna2 leads to the increased enzymatic activities, we expressed and purified both the HX-Dna2N (N-terminal 45 kDa domain) and the HX-Dna2Δ405N (Dna2 lacking the N-terminal 405 amino acids) proteins (Fig. 2A). The retarded migration of HX-Dna2N is due to the presence of additional amino acids containing polyhistidine and Xpress tags at its N-terminus (Fig. 2A). The isolated HX-Dna2N protein did not possess any detectable ATPase or endonuclease activity (data not shown). The isolated HX-Dna2Δ405N protein contained both ATPase and endonuclease activities (Fig. 2B and C). In keeping with the results obtained from the subtilisin digestion experiment, the specific activities of endonuclease and ATPase of Dna2Δ405N were significantly higher (~3- to 5-fold) than the full-length HX-Dna2 activities (Fig. 2B and C).

The hydrodynamic properties of HX-Dna2 and HX-Dna2Δ405N reveal that Dna2 is active as the monomer

Since Dna2 was previously reported to be active as a dimer (9), we measured the native molecular weight of HX-Dna2 and HX-Dna2Δ405N in order to determine whether deletion of the N-terminal region affected multimerization of Dna2. During glycerol gradient centrifugation the two proteins sedimented identically with a sedimentation coefficient of 5.9 *s*, although they differed significantly in molecular weights (Fig. 3A and C). Two possible explanations for this finding are (i) that the two molecules differ greatly in shape, which affects their sedimentation profiles, and (ii) that the HX-Dna2Δ405N protein multimerizes efficiently in the absence of the N-terminal 45 kDa domain, thus sedimenting with the same *s* value as full-length Dna2. In order to distinguish between these two possibilities, we carried out gel filtration chromatography and measured the Stokes radii of HX-Dna2 and HX-Dna2Δ405N (Fig. 3B). Gel filtration analyses revealed that HX-Dna2 and HX-Dna2Δ405N eluted at markedly different positions, yielding Stokes radii of 73.3 and 44.1 Å, respectively (Fig. 3B and C). Assuming a partial specific volume of 0.725 ml/g, HX-Dna2 was calculated to have a native molecular mass of 179 kDa and frictional ratio of 1.99 (Table 3) by the method of Siegel and Monty (18). HX-Dna2Δ405N had a native molecular mass of 108 kDa with a frictional ratio of 1.34 (Table 3). These results suggest that both wild-type HX-Dna2 and HX-Dna2Δ405N are monomeric proteins that differ in shape. Specifically, wild-type HX-Dna2 appears to possess a highly prolate shape, whereas the protein devoid of the N-terminal 45 kDa domain is spherical. This may account for the significant difference in the gel filtration profile but similar sedimentation pattern during glycerol gradient centrifugation. We obtained identical results when we performed hydrodynamic analyses under more physiological salt conditions (150 mM NaCl) as under high salt conditions (500 mM NaCl) (data not shown). In order to confirm that Dna2 does not form a dimer or higher ordered structure *in vivo*, we co-expressed two differentially tagged Dna2 proteins in insect cells, with a polyhistidine or hemagglutinin epitope fused to the N-terminus of Dna2 (HX-Dna2 and HA-Dna2, respectively). The extracts prepared from insect cells co-expressing the two Dna2 enzymes were passed through a Ni^{2+} column and the resulting fractions were examined by western blot analysis using anti-His or anti-HA monoclonal antibodies. The result is that the column retained HX-Dna2, but not HA-Dna2, regardless of the salt concentrations used throughout the chromatographic steps

(Fig. 4A and B), indicating that Dna2 does not form a complex with itself *in vivo*. This result, together with those from the hydrodynamic analyses above, demonstrates that Dna2 is monomeric both *in vivo* and *in vitro*, in contrast to a previous report (9). In addition, these results rule out the possibility that the *in vivo* defect associated with deletion of the N-terminal region of Dna2 (see below) is caused by an impaired ability to multimerize.

Deletion of the N-terminal 405 amino acids of Dna2 results in temperature-sensitive growth of mutant cells

In order to define the regions in *DNA2* that are dispensable for cell viability, we constructed plasmids that contained N-terminal deletions in *DNA2* lacking the first 105, 405 or 550 amino

acids of Dna2 (pRS314-dna2Δ105N, pRS314-dna2Δ105N and pRS314-dna2Δ550N, respectively). The plasmids were then introduced into YKH12 cells (deleted of chromosomal *DNA2* but harboring pRS316-DNA2; 10). In each case, expression of the mutant *dna2* allele was under control of its native chromosomal promoter. As shown in Figure 5A, all transformants that possessed both wild-type and mutant *dna2* alleles grew as efficiently as the wild-type control (left panel, –FOA) at 30°C. When the plasmid pRS316-DNA2, containing wild-type *DNA2*, was removed by growth in the presence of 5′-FOA (right panel, +FOA), the mutant alleles *dna2Δ105N* and *dna2Δ405N* supported cell growth (Fig. 5A, +FOA), consistent with the fact that Dna2Δ405N possesses both endonuclease and ATPase activities crucial for cell viability (9,10,19). In contrast, the *dna2Δ550N* allele did not support cell growth in the absence of wild-type Dna2 protein (Fig. 5A). This result is consistent with the previous result that the deletion of 550 amino acids includes the region critical for endonuclease activity that is essential for cell viability (8,10).

Since variations in the copy number and in expression levels of genes on plasmids could have affected cell viability in the above plasmid shuffling experiment, we replaced the chromosomal *DNA2* with either the *dna2Δ105N* or *dna2Δ405N* allele for a more conclusive analysis. Interestingly, strains carrying a single copy of either the *dna2Δ105N* or *dna2Δ405N* mutant allele showed temperature-dependent growth (Fig. 5B), similar to a control temperature-sensitive allele, *dna2-1* (2). This result indicates that deletion of the N-terminal 405 amino acids causes a defect in the function of *DNA2 in vivo*.

Unlike many identified *dna2* mutant alleles that are sensitive to the alkylating agent MMS, cells containing *dna2Δ405N* were not sensitive to MMS (data not shown). To date, none of the previously identified mutant *dna2* alleles rendered cells UV sensitive, suggesting that *DNA2* is unlikely to participate in the repair of UV-damaged DNA. However, both *dna2Δ405N* and *dna2Δ105N* mutant cells were found to be weakly sensitive to UV. Mutant cells were most susceptible to UV at a dose of 25 J/m² (Fig. 5C), suggesting that the N-terminal region may play a role in UV-induced DNA damage repair.
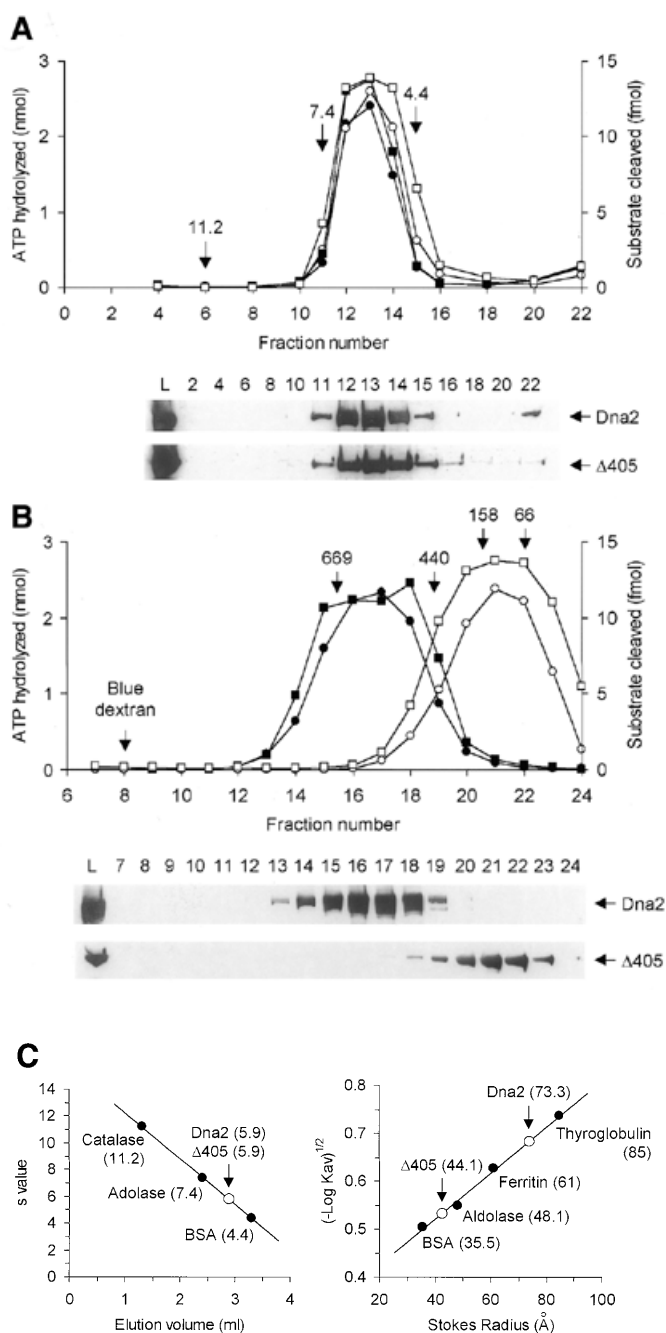

Figure 3. Dna2 is active as a monomer and removal of the N-terminal 45 kDa renders the enzyme spherical. (**A** and **B**) Purified HX-Dna2 (50 μg) and HX-Dna2Δ405N (50 μg) were subjected to glycerol gradient centrifugation (A) and gel filtration (B) as described in Materials and Methods. ATPase (circles) and endonuclease (squares) activities of HX-Dna2 (closed symbols) and HX-Dna2Δ405N (open symbols) were measured across the glycerol gradient (200 μl) and gel filtration fractions (60 μl) (top of each figure). The material subjected to these steps (indicated by L) and the resulting fractions (2 μl) were subjected to 8% SDS–PAGE and then analyzed by western blotting using α-Dna2 polyclonal antibodies (bottom of each figure). The marker proteins used for glycerol gradients were catalase (11.2 S), aldolase (7.4 S) and BSA (4.4 S) and their sedimentation positions are indicated by arrows. The size markers used for gel filtration were thyroglobulin (669 kDa, 85 Å), ferritin (440 kDa, 61 Å), aldolase (158 kDa, 48.1 Å) and BSA (66 kDa, 35.5 Å). Elution positions of the marker molecules as well as blue dextran were as indicated. (**C**) Sedimentation values (left) and Stokes radii (right) of the two Dna2 enzymes were determined from (A) and (B), respectively. The Stokes radii of the two Dna2 enzymes were determined by plotting the Stokes radii (Å) of marker molecules against (−logK_{av})^{1/2}.
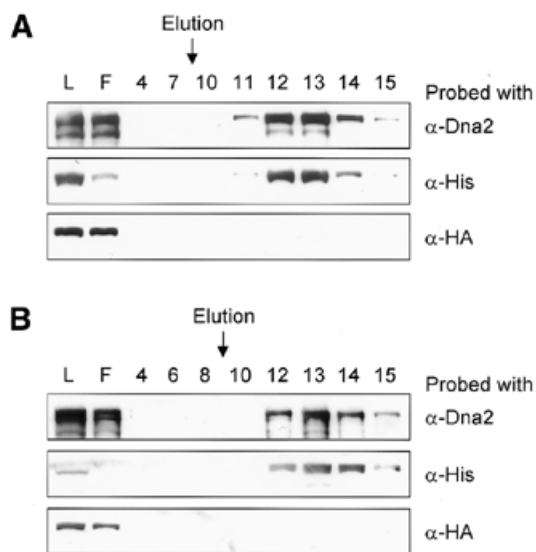
Figure 4. Dna2 does not dimerize *in vivo*. Crude extracts (570 mg) were prepared from insect cells (1 l) co-infected with recombinant baculoviruses expressing either histidine-tagged Dna2 (HX-Dna2) or hemagglutinin-tagged Dna2 (HA-Dna2). Dna2 protein enriched on a heparin–Sepharose column was dialyzed against buffer T (25 mM Tris–HCl, pH 7.5, 10% glycerol, 0.02% Nonidet P-40). The dialysate was adjusted to either 150 (**A**) or 500 (**B**) mM NaCl and placed on a Ni^{2+}–NTA–agarose column. The column was eluted with buffer T plus 400 mM imidazole containing the same concentrations of salt [for (A) 150 mM and for (B) 500 mM] as the load materials. The load (L, 10 µg), flow-through (F, 10 µg) and Ni^{2+} column fractions (1 µl) were subjected to 8% SDS−PAGE and analyzed by western blot using polyclonal antibodies specific for Dna2 (α-Dna2) and monoclonal antibodies specific for the polyhistidine (α-His) and hemagglutinin (α-HA) epitopes.

The temperature-dependent growth defect is suppressed either by slowing the growth rate or by overexpressing the mutant allele itself or wild-type *RAD27*

We found that *dna2Δ405N* cells had a severe growth defect at 37°C (Fig. 6A). However, the presence of 20 mM hydroxyurea, a concentration insufficient to arrest cells in S phase but which retards growth of wild-type cells, partially restored the growth of mutant cells at 37°C (Fig. 6A). In addition, cells were able to grow at 37°C when the carbon source was switched from dextrose to glycerol/lactate. Under these conditions cells doubled ~2-fold more slowly than cells grown in the presence of glucose (data not shown). This suggested that the enzymatic activities associated with the Dna2Δ405N enzyme *in vivo* were not sufficient to support rapid cell growth. Overexpression of Dna2Δ405N or Rad27, but not the N-terminal 405 amino acid fragment, rescued the temperature-sensitive phenotype of *dna2Δ405N* mutant cells (Fig. 6B). This is consistent with the idea that the mutant enzyme does not function optimally and, thus, the mutant cells might require higher levels of endonuclease activity to grow normally. Alternatively, the fact that elevated levels of Dna2Δ405N itself can rescue the temperature-dependent lethality of *dna2Δ405N* may suggest that deletion of the N-terminal region reduces levels of the mutant enzyme by decreasing either expression level or stability. This is not likely, however, since we used the native
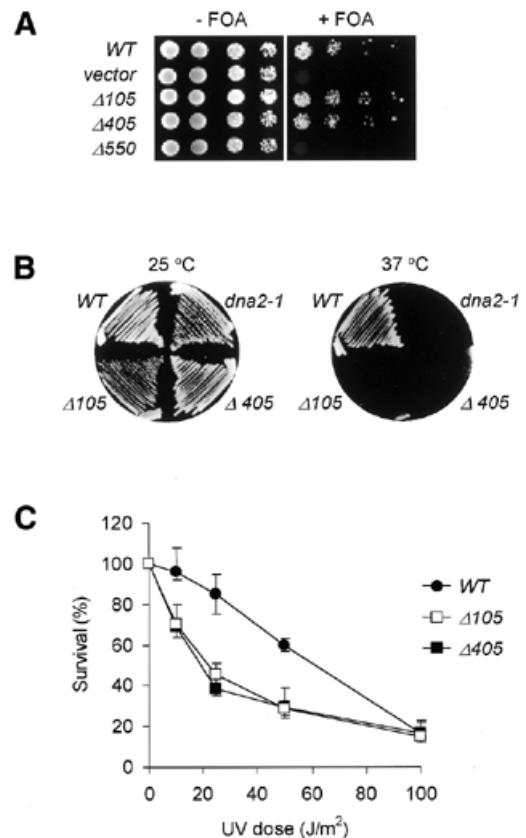

Figure 5. The *dna2Δ405N* mutant displays a temperature-sensitive growth phenotype and is moderately sensitive to UV irradiation. (**A**) Strain YKH12 was transformed with one of pRS314-DNA2 (*WT*), pRS314-Dna2Δ105N (*Δ105*), pRS314-Dna2Δ405N (*Δ405*), pRS314-Dna2Δ550N (*Δ550*) or pRS314 vector alone (*vector*). Ten-fold serial dilutions of each transformant were spotted onto complete synthetic medium lacking tryptophan in the absence (–FOA) or presence (+FOA) of 5-FOA. Cells were grown at 30°C for 3 days. (**B**) Temperature-sensitive growth defect of N-terminal deleted *dna2* mutant cells. Strains containing the wild-type *DNA2* (*WT*), *dna2Δ105N* (*Δ105N*), *dna2-Δ405N* (*Δ405N*) or *dna2-1* (2) allele were streaked onto rich medium in duplicate and grown for 3 days at 25 and 37°C. (**C**) *dna2Δ405N* mutants are sensitive to UV irradiation. Cells containing the wild-type *DNA2* (*WT*) (YPH499), *dna2Δ105N* (*Δ105*) (YJA7) or *dna2Δ405N* (*Δ405*) (YJA2) alleles were plated onto rich medium and irradiated with UV as indicated. The number of viable colonies formed at 25°C was counted to measure survival.

promoter to drive expression of both enzymes and removal of the unstructured N-terminal 405 amino acids tends to make the mutant enzyme more resistant to proteolysis, hence increasing its stability.

The N-terminal 45 kDa domain interacts physically with the central region of Dna2 located between the nuclease and helicase domains

Deletions of the N-terminus of Dna2 up to 405 amino acids resulted in temperature-sensitive growth of mutant cells. This observation raised the possibility that the N-terminal 45 kDa fragment may regulate the enzymatic activities of Dna2. The N-terminal domain may interact intramolecularly with other domains of Dna2 and thereby induce a conformational change in the catalytic domains. This intramolecular interaction may
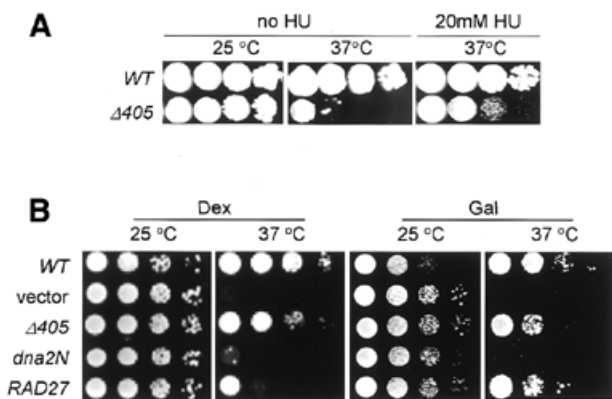
Figure 6. The defect associated with the N-terminal 45 kDa deletion is rescued by overexpression of the mutant allele itself or a functional *RAD27* gene. (**A**) Temperature sensitivity of the *dna2Δ405N* mutation is suppressed when growth is retarded. Ten-fold serial dilutions of liquid cultures of wild-type (*WT*) and *dna2Δ405N* (*Δ405*) strains were spotted onto solid medium in the absence (no HU) or presence (20 mM HU) of hydroxyurea and the cells were grown for 5 days at 25 and 37°C. (**B**) Suppression of the temperature-sensitive phenotype of the *dna2Δ405N* mutant allele. The temperature-sensitive phenotype of the *dna2Δ405N* mutant strain is suppressed by overexpressing either Dna2Δ405N (*Δ405*) or Rad27 (*RAD27*) protein, but not by the N-terminal 45 kDa domain (*dna2N*). The *dna2Δ405N* mutant (YJA2) strain was transformed with pYES2 alone (*vector*) or pYES2-derived plasmids expressing either wild-type Dna2 (*WT*), Dna2Δ405N (*Δ405*), the N-terminal 405 amino acid domain (*dna2N*) or yeast Fen1 (*RAD27*). Liquid cultures of the resulting transformants were serially diluted and spotted in duplicate onto rich medium containing either dextrose (Dex) or galactose (Gal) and grown for 3 or 5 days, respectively, at 25 and 37°C.

also be regulated intermolecularly by other proteins. In order to explore this possibility, we determined whether purified HX-Dna2N (the N-terminal 405 amino acid fragment) inhibited the enzymatic activities of N-terminal deleted Dna2Δ405N *in trans*. No effect, however, was detected *in vitro* (data not shown). This is consistent with the *in vivo* observation that the N-terminal region of Dna2 did not rescue the temperature-sensitive growth defect of *dna2Δ405N* mutant cells (Fig. 6B). These results suggest that the N-terminal region of Dna2 acts *in cis* with the catalytic domain of Dna2.

We then searched for intramolecular interactions within Dna2 in two different ways. First, we investigated interactions *in vivo* using the yeast two-hybrid assay. For this purpose, the N-terminal 45 kDa domain encoded by the *Bam*HI–*Nde*I fragment (1214 bp) was fused to the *GAL4* DNA-binding domain and used as bait (Fig. 7A). In order to search for an intra-molecular interacting partner, we constructed six different prey vectors expressing truncated proteins encoded by restriction fragments of *DNA2*: *Nde*I (1214)–*Pvu*II (2975), *Stu*I (2080)–*Stu*I (3867), *Pvu*II (2975)–*Bam*HI (4782), *Nde*I (1214)–*Stu*I (2080), *Sac*II (1596)–*Bgl*I (2558) and *Stu*I (2080)–*Eco*RV (2920) (numbers in parentheses indicate positions of restriction sites) (Fig. 7A). Transformants containing both the bait and one of the above prey vectors were examined for growth on plates containing 30 mM 3-aminotriazole, which scores for bait–prey interactions *in vivo*. Yeast cells expressing truncated proteins from *Nde*I (1214)–*Pvu*II (2975), *Stu*I (2080)–*Stu*I (3867), *Sac*II (1596)–*Bgl*I (2558) or *Stu*I (2080)–*Eco*RV (2920) yielded viable colonies, whereas cells expressing the truncated proteins from *Pvu*II (2975)–*Bam*HI (4782) or *Nde*I
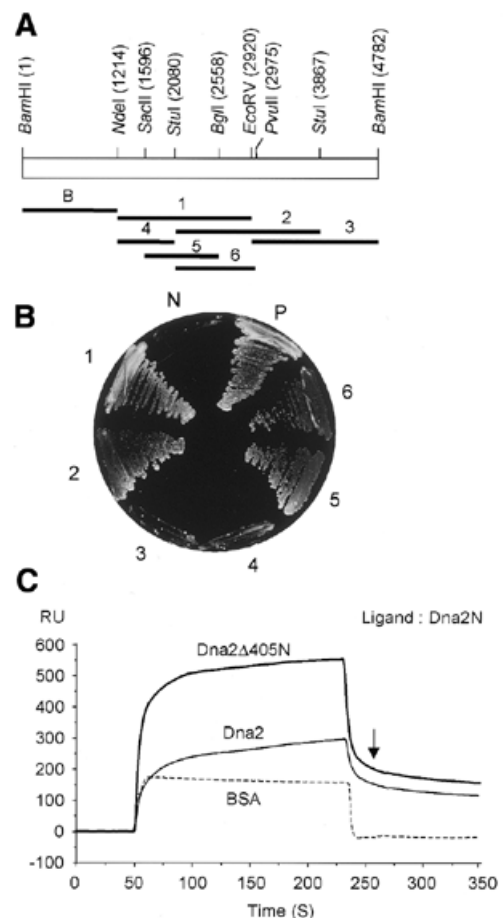
Figure 7. Intramolecular interaction of the N-terminal 405 amino acid fragment with a central region of Dna2 located between the endonuclease and ATPase domains. (**A**) Restriction enzyme sites in the yeast *DNA2* open reading frame that were used to construct plasmids for yeast two-hybrid analyses. The numbers in parentheses indicate the nucleotide position of each restriction enzyme. The bold bars indicate the fragments cloned into yeast two-hybrid vectors. The B fragment containing the N-terminal 405 amino acids was used as bait. The fragments indicated by the numbers 1–6 were used as prey. (**B**) Yeast two-hybrid analyses. Cells harboring the bait vector were transformed with six different prey vectors (indicated by the numbers 1–6). The transformants obtained were streaked onto synthetic dropout (SD) minimal medium lacking L-histidine and examined for their ability to grow in the presence of 30 mM 3-aminotriazole. Yeast cells harboring the prey vector (pACT2) were used as a negative control (indicated by N). P indicates a positive control provided by the manufacturer to show the interaction between simian virus 40 T antigen and p53. (**C**) Physical interaction between HX-Dna2N and HX-Dna2Δ405N detected by surface plasmon resonance analysis. The rate of increase in ΔRU, the change in refractory index units (RU), after injection of solutions containing equimolar concentrations of wild-type HX-Dna2 (100 µg/ml; thin line), HX-Dna2 Δ405N (70 µg/ml; thick line) and BSA (250 µg/ml; dotted line) onto a Biosensor chip with immobilized HX-Dna2N is plotted. The arrow indicates the time point (~25 s after starting washing the chip with a buffer containing no protein) at which stable ΔRU values (200 for Dna2Δ405N and 150 for Dna2) were measured.

(1214)–*Stu*I (2080) did not (Fig. 7B). The negative result obtained with these two fragments was not due to lack of protein expression, since the fusion proteins were efficiently expressed in the cells as judged by western blot analyses (data not shown). These results suggest that the internal region spanning amino acids 693–853 in *DNA2* is sufficient to support the interaction with the N-terminal 45 kDa domain. This region is

roughly located between the two catalytic domains responsible for the endonuclease and ATPase/helicase activities of Dna2 (9,10). In order to confirm direct protein–protein interactions of HX-Dna2N with either wild-type HX-Dna2 or HX-Dna2Δ405N, surface plasmon resonance assays were carried out with a BIAcore instrument. As shown in Figure 7C, interactions were observed when equivalent levels (0.78 μM) of either HX-Dna2 or HX-Dna2Δ405N were passed over the surface of a chip on which HX-Dna2N was immobilized. The increases in refractory index, ΔRU, did not differ significantly (150 and 200, respectively). However, the initial binding rate was more efficient with Dna2Δ405N than with HX-Dna2, indicating that HX-Dna2N binds to Dna2Δ405N more rapidly than to HX-Dna2. This result, together with the results obtained from the yeast two-hybrid analyses, demonstrates that the N-terminal 45 kDa domain has an intramolecular interaction within Dna2.

Although an interaction between the N-terminal 45 kDa fragment and the Dna2Δ405 protein was detected in the two different assays, we failed to observe a stable complex between the two proteins during glycerol gradient sedimentation (data not shown). We interpret this result as meaning that the weak intramolecular interaction between the N-terminal and catalytic domains of Dna2 is required to facilitate a dynamic and reversible binding of a regulatory molecule to the N-terminal region (see below).

DISCUSSION

In this report we present evidence that the 172 kDa Dna2 protein consists of at least three structural domains by analyzing subtilisin-proteolyzed products formed *in vitro* and the phenotypes of cells producing corresponding mutant proteins *in vivo*. These results, together with those obtained from site-specific mutagenesis described elsewhere (9,10,19), demonstrate that each structural domain plays a distinct role in the multifunctional activities of Dna2: the central domain, encompassing approximately amino acid positions 500–760, encodes the endonuclease activity (8–10) and the C-terminal domain, located between amino acids 1050 and 1500, encodes the ATPase/helicase activity (7,19). The analyses of mutant Dna2 lacking the N-terminal 45 kDa region or mutant cells carrying an N-terminal 45 kDa deletion of Dna2 gave rise to particularly interesting results. (i) Removal of the N-terminal 45 kDa domain did not result in loss of either endonuclease or ATPase activity, thus being dispensable for the enzymatic activities of Dna2 (Figs 1 and 2). (ii) Rather, it increased the specific activity of the Dna2 enzyme *in vitro*. (iii) Despite the increased activities of the mutant enzyme, removal of the N-terminal region of Dna2 caused a severe growth defect *in vivo* (Fig. 5B). (iv) Overexpression of Dna2Δ405N suppressed its own temperature-sensitive growth defect (Fig. 6B). This indicates that deletion of the N-terminal region impairs proper functioning of Dna2 *in vivo*, although it has a higher specific activity of both endonuclease and ATPase than wild-type Dna2. One conceivable defect is that the N-terminal-deleted mutant protein is not properly targeted to the place where Okazaki fragment processing occurs. The other possible defect is that the enzyme activities of the mutant Dna2 protein are not properly implemented in the absence of the N-terminal
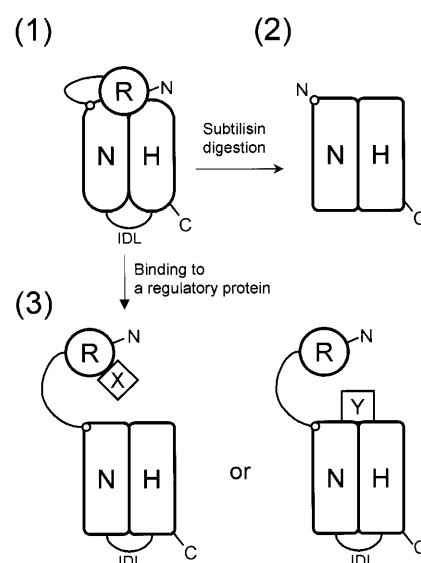
Figure 8. A model of the domain structure of Dna2 and its possible mode of regulation. In this model Dna2 consists of three main domains: one potential regulatory domain (indicated by R) and two catalytic domains (indicated by N and H) for endonuclease and ATPase/helicase activities, respectively. The N- and C-termini of Dna2 are indicated by N and C, respectively. IDL denotes the interdomain loop that connects the two catalytic domains. The small circle in the left upper corner of the endonuclease domain denotes the position of amino acid 405 of Dna2. (1) The N-terminal regulatory domain suppresses enzyme activity when it is associated intramolecularly with the region between the two catalytic domains of Dna2. (2) Subtilisin treatment destroys the N-terminal 45 kDa regulatory domain and the interdomain loop. This digestion changes the overall shape of Dna2 from a prolate to a spherical molecule. Removal of the regulatory domain is accompanied by a conformational change in the catalytic domains, increasing the enzymatic activities of Dna2. (3) The N-terminal domain is a target for regulation and is displaced by other proteins (indicated by molecules X and Y) through protein–protein interactions in two different modes, as depicted. This interaction not only activates the enzymatic activities of Dna2 by inducing a conformational change in the catalytic domains, but might also target the enzyme to the location where Okazaki fragment processing occurs.

region. We prefer the latter possibility for the reasons discussed below.

As depicted in Figure 8, we propose a model that summarizes the structure of Dna2 and the possible regulation of its function. The main feature of this model is that Dna2 acts as a monomer and contains two essential catalytic domains that are regulated by the N-terminal 45 kDa region. This model is based upon the following results. (i) The N-terminal 45 kDa domain was rapidly degraded by subtilisin, whereas the C-terminal region of Dna2 was resistant to proteolysis. This suggests that the N-terminal region may be relatively unstructured and easily accessible to a non-specific protease such as subtilisin. (ii) The remaining C-terminal 127 kDa region may be more compact structurally and more resistant to proteolysis. However, digestion with increasing amounts of subtilisin converted the 127 kDa polypeptide into two fragments of similar size, 58 and 60 kDa, indicating that cleavage occurred approximately in the middle of the polypeptide. Thus, the two compact catalytic domains appear to be connected by a small interdomain loop cleavable by increased levels of subtilisin. Further cleavage of the 127 kDa polypeptide did not destroy

either the ATPase or endonuclease activities of Dna2. (iii) The 45 kDa N-terminal domain of Dna2 interacts intramolecularly with the central region of Dna2 that lies between the two catalytic domains. It is conceivable that the N-terminal domain is dislodged with the aid of a protein(s) that acts in concert with Dna2 during Okazaki fragment elongation and processing *in vivo*. If this is the case, our model predicts the existence of regulatory protein factors as depicted in Figure 8 that might activate and target Dna2 to places at which Okazaki fragment processing occurs.

As a first attempt to identify such a potential regulatory factor for Dna2, we tested whether purified Rad27 of yeast could alter the enzymatic activity of Dna2, since *RAD27* is known to interact with *DNA2* both genetically and physically *in vivo* (11). However, purified Rad27 enzyme neither stimulated nor inhibited the enzyme activities of Dna2 (data not shown) and we were not able to detect any stable complex formation between these purified proteins (17). This led us to continue to search for putative regulatory factors of Dna2. For this purpose we screened for suppressors that restored the temperature-sensitive growth phenotype of cells carrying mutant *DNA2* lacking the N-terminal 405 amino acids. One suppressor isolated was *RFA2*, which encodes the 34 kDa middle subunit of replication protein A (RPA) (20). In subsequent analyses the two other subunits, *RFA1* and *RFA3*, also suppressed the temperature growth defect of *dna2Δ405N* mutant cells. We believe that expression of one subunit of RPA induces compensatory expression of the other two subunits, accounting for suppression of the temperature-sensitive growth defect by all three subunits. Examining the influence of RPA on Dna2 revealed that intact RPA had differential effects on the endonuclease activity of Dna2 depending on the types of ssDNA used. RPA inhibited the cleavage of ssDNA flanked by partial DNA duplexes, but markedly stimulated cleavage of the free ssDNA 5′-tail (1,20). The interaction of RPA and Dna2 was found to play an important role in processing of Okazaki fragments by controlling the endonuclease switch between Dna2 and Fen1 (20). Further characterization of the physical interaction between Dna2 and RPA revealed that Dna2 interacts with RPA mainly through RFA1, the large subunit of RPA (manuscript in preparation). Two modes of interaction between RFA1 and Dna2 were noted: the primary interaction occurred between the C-terminal regions of both proteins and the secondary interaction required the N-terminal regions of both proteins (RFA1, amino acids 1–180; Dna2, amino acids 1–405). Dna2 lacking the N-terminal 45 kDa fragment required more RPA to be activated to comparable levels to wild-type Dna2, accounting for the mechanism by which RPA suppresses the temperature-sensitive growth defect caused by deletion of the N-terminal 45 kDa region. Conversely, RPA containing the mutant RFA1 subunit devoid of the N-terminal amino acids 1–180 failed to fully stimulate the endonuclease activity of intact Dna2, verifying the functional importance of the secondary interaction. Thus, the primary role of the Dna2 N-terminus appears to be to mediate the RPA interaction required for optimal implementation of the enzymatic activities of Dna2.

Interestingly, both the Dna2 proteins isolated from fission and budding yeasts contain additional 300–400 amino acid sequences at their N-termini that are not found in higher

eukaryotes, including *Arabidopsis thaliana*, *Xenopus laevis*, *Caenorhabditis elegans* and humans (2,5,6,10). The N-terminal regions of Dna2 from the two yeasts are not conserved and are devoid of any motifs that could reveal their function (2,5). This suggests that the non-conserved N-terminal region from unicellular eukaryotes may have a regulatory role that may be species-specific in lower eukaryotes. In keeping with this possibility, *S.pombe cdc24+*, a novel replication gene essential for chromosome integrity a structural equivalent of which is lacking in *Saccharomyces cerevisiae* (21), specifically interacts with the N-terminal part of *S.pombe dna2+* in the yeast two-hybrid assay (data not shown). The N-terminal regions of *S.cerevisiae* Dna2 may be functionally replaced *in trans* with other proteins in higher eukaryotes.

ACKNOWLEDGEMENTS

REFERENCES

1. Bae,S.H. and Seo,Y.S. (2000) Characterization of the enzymatic properties of the yeast dna2 helicase/endonuclease suggests a new model for Okazaki fragment processing. *J. Biol. Chem.*, **275**, 38022–38031.
2. Budd,M.E. and Campbell,J.L. (1995) A yeast gene required for DNA replication encodes a protein with homology to DNA helicases. *Proc. Natl Acad. Sci. USA*, **92**, 7642–7646.
3. Budd,M.E. and Campbell,J.L. (2000) The pattern of sensitivity of yeast dna2 mutants to DNA damaging agents suggests a role in DSB and postreplication repair pathways. *Mutat. Res.*, **459**, 173–186.
4. Formosa,T. and Nittis,T. (1999) Dna2 mutants reveal interactions with DNA polymerase alpha and Ctf4, a Pol alpha accessory factor and show that full Dna2 helicase activity is not essential for growth. *Genetics*, **151**, 1459–1470.
5. Kang,H.Y., Choi,E., Bae,S.H., Lee,K.H., Gim,B.S., Kim,H.D., Park,C., MacNeill,S.A. and Seo,Y.S. (2000) Genetic analyses of *Schizosaccharomyces pombe dna2+* reveal that Dna2 plays an essential role in Okazaki fragment metabolism. *Genetics*, **155**, 1055–1067.
6. Liu,Q., Choe,W.C. and Campbell,J.L. (2000) Identification of the *Xenopus laevis* homolog of *Saccharomyces cerevisiae* DNA2 and its role in DNA replication. *J. Biol. Chem.*, **275**, 1615–1624.
7. Bae,S.H., Choi,E., Park,J.S., Lee,S.H., Lee,K.H. and Seo,Y.S. (1998) Dna2 of *Saccharomyces cerevisiae* possesses a single-stranded DNA-specific endonuclease activity that is able to act on double-stranded DNA in the presence of ATP. *J. Biol. Chem.*, **273**, 26880–26890.
8. Aravind,L., Walker,D.R. and Koonin,E.V. (1999) Conserved domains in DNA repair proteins and evolution of repair systems. *Nucleic Acids Res.*, **27**, 1223–1242.
9. Budd,M.E., Choe,W.C. and Campbell,J.L. (2000) The nuclease activity of the yeast DNA2 protein, which is related to the RecB-like nucleases, is essential *in vivo*. *J. Biol. Chem.*, **275**, 16518–16529.
10. Lee,K.H., Kim,D.W., Bae,S.H., Kim,J.A., Ryu,G.H., Kwon,Y.N., Kim,K.A., Koo,H.S. and Seo,Y.S. (2000) The endonuclease activity of the yeast Dna2 enzyme is essential *in vivo*. *Nucleic Acids Res.*, **28**, 2873–2881.
11. Budd,M.E. and Campbell,J.L. (1997) A yeast replicative helicase, Dna2 helicase, interacts with yeast FEN-1 nucleases in carrying out its essential function. *Mol. Cell. Biol.*, **17**, 2136–2142.
12. Braguglia,D., Heum,P., Pasero,P., Duncker,B.P. and Gasser,S.M. (1998) Semi-conservative replication in yeast nuclear extracts requires Dna2 helicase and supercoiled template. *J. Mol. Biol.*, **281**, 631–649.
13. Fiorentino,D.F. and Crabtree,G.R. (1997) Characterization of *Saccharomyces cerevisiae* dna2 mutants suggests a role for the helicase late in S phase. *Mol. Biol. Cell*, **8**, 2519–2537.

14. Parenteau,J. and Wellinger,R.J. (1999) Accumulation of single-stranded DNA and destabilization of telomeric repeats in yeast mutant strains carrying a deletion of *RAD27*. *Mol. Cell. Biol.*, **19**, 4143–4152.
15. Singer,M.S., Kahana,A., Wolf,A.J., Meisinger,L.L., Peterson,S.E., Goggin,C., Mahowald,M. and Gottschling,D.E. (1998) Identification of high copy disruptors of telomeric silencing in *Saccharomyces cerevisiae*. *Genetics*, **150**, 613–631.
16. Park,J.S., Choi,E., Lee,S.H., Lee,C. and Seo,Y.S. (1997) A DNA helicase from *Schizosaccharomyces pombe* stimulated by single-stranded DNA-binding protein at low ATP concentration. *J. Biol. Chem.*, **272**, 18910–18919.
17. Bae,S.H. and Seo,Y.S. (2000) *In vitro* evidence that purified yeast Rad27 and Dna2 are not stably associated with each other suggests that an additional protein(s) is required for a complex formation. *J. Biochem. Mol. Biol.*, **33**, 155–161.
18. Siegel,L.M. and Monty,K.J. (1966) Determination of molecular weights and frictional ratios of proteins in impure systems by use of gel filtration and density gradient centrifugation. Application to crude preparations of sulfite and hydroxylamine reductases. *Biochim. Biophys. Acta*, **112**, 346–362.
19. Budd,M.E., Choe,W.C. and Campbell,J.L. (1995) DNA2 encodes a DNA helicase essential for replication of eukaryotic chromosomes. *J. Biol. Chem.*, **270**, 26766–26769.
20. Bae,S.H., Bae,K.H., Kim,J.A. and Seo,Y.S. (2001) RPA-governed endonuclease switching during Okazaki fragment processing. *Nature*, in press.
21. Gould,K.L., Burns,C.G., Feoktistova,A., Hu,C.P., Paison,S.G. and Forsburg,S.L. (1998) Fission yeast *cdc24*+ encodes a novel replication factor required for chromosome integrity. *Genetics*, **149**, 1221–1233.